


Article

Screening of Key Indices and the Gene Transcriptional Regulation Analysis Related to Salt Tolerance in *Salix matsudana* Seedlings

Yuanxiang Pang ¹ , Longmei Guo ¹, Tiantian Wang ^{1,2}, Wei Liu ¹, Peili Mao ¹, Xiaonan Cao ¹, Ying Geng ¹ and Banghua Cao ^{1,*}

- ¹ Taishan Mountain Forest Ecosystem Research Station, Key Laboratory of State Forestry Administration for Silviculture of the Lower Yellow River, Shandong Agricultural University, Tai'an 271018, China; pangyuanxiang2020@126.com (Y.P.); guolm3180@126.com (L.G.); wtt840602@163.com (T.W.); liucw2022@126.com (W.L.); maopl1979@163.com (P.M.); caoxiaonan_05@163.com (X.C.); aimee_gy@163.com (Y.G.)
- ² Dongying Landscaping Center (Shandong), Dongying 257091, China
- * Correspondence: caobanghua@126.com

Abstract: Pot experiments were performed to comparatively study the differences in 16 salt tolerance indices between the seedlings of six *Salix matsudana* clones under the stress of various concentrations of NaCl (0, 0.1%, 0.3%, 0.5%, and 0.7%), including the salt injury index, shoot fresh weight, root fresh weight, leaf water content, relative conductivity, malondialdehyde content, and antioxidant enzyme activity. The salt-tolerant clones and key indices of salt tolerance were selected. Transcriptome sequencing analysis was performed on the selected salt-tolerant and salt-sensitive clones under salt stress, and the links between the physiological indices of salt tolerance and gene expression were analyzed. Results: (1) Superoxide dismutase (SOD), peroxidase (POD), chlorophyll, and net photosynthetic rate were closely related to the salt tolerance of *Salix matsudana* at the seedling stage. The regression equation was constructed as follows: salt tolerance index (y) = $0.224x_{10} + 0.216x_{11} + 0.127x_{12} + 0.191x_7 - 0.187$ (x_{10} = chlorophyll, x_{11} = SOD, x_{12} = POD, x_7 = net photosynthetic rate). (2) The number of differentially expressed genes between the seedlings of salt-tolerant and salt-sensitive clones varied with the time of exposure (0 h, 4 h, 12 h, and 24 h) to 200 mmol·L⁻¹ NaCl stress. The most differentially expressed genes in Sm172 were detected upon 24 h vs. 4 h of salt treatment, while the most in Sm6 were in the 24 h vs. 0 h comparison. Gene Ontology analysis and Kyoto Encyclopedia of Genes and Genomes analysis showed that several differentially expressed genes were involved in carotenoid biosynthesis and plant mitogen-activated protein kinase signaling pathways. The nine highly expressed transcription factor genes (*Sm172-f2p30-2392*, *Sm172-f2p28-2386*, *Sm6-f8p60-2372*, *Sm6-f2p39-2263*, *Sm6-f16p60-2374*, *Sm6-f3p60-931*, *Sm6-f2p60-1067*, *Sm172-f3p54-1980*, and *Sm172-f3p54-1980*) were closely correlated with the four key indices of salt tolerance. These genes could become genetic resources for salt tolerance breeding of *Salix matsudana*.

Keywords: *Salix matsudana*; NaCl stress; salt tolerance index; salt tolerance gene; transcriptome sequencing



Citation: Pang, Y.; Guo, L.; Wang, T.; Liu, W.; Mao, P.; Cao, X.; Geng, Y.; Cao, B. Screening of Key Indices and the Gene Transcriptional Regulation Analysis Related to Salt Tolerance in *Salix matsudana* Seedlings. *Forests* **2022**, *13*, 754. <https://doi.org/10.3390/f13050754>

Academic Editor: Claudia Cocozza

Received: 2 April 2022

Accepted: 11 May 2022

Published: 13 May 2022

Publisher's Note: MDPI stays neutral with regard to jurisdictional claims in published maps and institutional affiliations.



Copyright: © 2022 by the authors. Licensee MDPI, Basel, Switzerland. This article is an open access article distributed under the terms and conditions of the Creative Commons Attribution (CC BY) license (<https://creativecommons.org/licenses/by/4.0/>).

1. Introduction

The coastal saline-alkali land of the Yellow River Delta suffers frequent natural disasters, soil salinization, and great difficulty in afforestation, which restricts the growth of many tree species [1–3]. The selection of salt-tolerant afforestation tree species is a key measure to improving the outcome of afforestation. Willow (*Salix matsudana*) is a native arbor species naturally distributed in this area that has a certain tolerance to salt. Selection and breeding of improved willow varieties could greatly help with the construction of shelter forests in the Yellow River Delta.

Early studies on salt resistance in willows have focused on their salt resistance ability and physiological characteristics. *Salix matsudana* can grow in a culture medium with a NaCl concentration of 0.1–0.2 g L⁻¹, whereas the salt stress caused by 0.4 g L⁻¹ NaCl significantly inhibits its growth [4]. Salt stress damages the stems and leaves of willow [5]; reduces its growth increment, biomass, and leaf water content [6]; and causes ion toxicity, osmotic stress, and secondary oxidative stress to the plant, thereby hindering its photosynthesis, growth, and metabolism [7]. When osmotic stress occurs, osmotic adjustment substances (soluble sugars and soluble proteins) accumulate in plant cells to maintain a higher water potential [8,9]. Osmotic stress and the toxicity of excessive Na⁺ will cause the accumulation of reactive oxygen species in plants [10]. The antioxidant enzyme system (including superoxide dismutase (SOD) and peroxidase (POD)) in plants will be activated [11], which scavenges peroxide ions and reduces the oxidative damage to the cells [12,13].

As molecular biology techniques have advanced, research on the salt tolerance of willows has advanced to the molecular level. Qiao et al. analyzed the salt-stress-responsive proteome of *Salix matsudana* [14]. Zhou et al. discovered significantly different miRNA expressions between salt-sensitive and salt-tolerant *Salix matsudana* under various salt stress conditions [15]. Chen et al. identified candidate genes for salt stress response in *Salix matsudana* [16]. Shan et al. found that the physiological and metabolic processes of plants could be regulated by controlling salt-stress-related genes [17]. Yang et al. [18] found that in a high-salt environment, the upregulation of H⁺-ATPase gene expression in vacuoles led to cytoplasmic sequestration of Na⁺ [19]. Plants also respond to salt stress by regulating the expression of salt-tolerance-related transcription factors such as WRKY, MYB, and basic helix-loop-helix (BHLH) [20–22].

With the gradual maturation of sequencing technology, research based on transcriptome sequencing has expanded from animals to plants. Transcriptomic research in plants has mainly focused on stress resistance, regulation of physiological mechanisms, and nutrient utilization. Studies on stress resistance mainly focus on salt and alkali tolerance, disease resistance, and drought resistance [23–26]. Transcriptome sequencing plays an increasingly important role in mining the salt tolerance genes of plant species, such as *Jatropha curcas*, citrus, cotton, wheat, and rose [27–32]. The application of third-generation single-molecule sequencing technology reduces the difficulty of analyzing the nonparametric transcriptome and allows for the easy sequencing of the complete genome and full-length transcripts, making the in-depth study of transcription mechanisms more convenient. However, there have been few studies on the relationship between the physiological salt-stress-responsive indices and the molecular mechanism of salt tolerance that have used third-generation sequencing technology and have applied the findings to the breeding of salt-tolerant varieties.

The present study examined 16 salt-tolerance-related indices in seedlings of *Salix matsudana*. On this basis, correlation analysis, grey cluster analysis, principal component analysis, and stepwise regression analysis were performed to screen out the key indices, pick the salt-tolerant and salt-sensitive *Salix matsudana* clones, and derive the equation that accurately reflected the salinity resistance of *Salix matsudana*. Transcriptome analysis was carried out on the selected salt-tolerant and salt-sensitive clones. The pathways involved in the salt tolerance of *Salix matsudana* and their relevant genes were identified on the basis of the differentially expressed genes and the key indices of salt tolerance. Eventually, an identification method of salt tolerance that was stable and efficient in both the physiological and molecular aspects was established for *Salix matsudana* at the seedling stage. This study might provide a theoretical and technical basis for the selection and breeding of improved varieties that can tolerate the salinity of coastal saline-alkali land.

2. Materials and Methods

2.1. Experimental Materials

The research objects included a total of five willow clones: the improved salt-tolerant varieties Luliu 2 and Luliu 6, which were registered by the Shandong Academy of Forestry

Sciences, as well as three unapproved clones with good traits (preliminarily named Jinan 1, Jinan 2, and Binzhou 1) in the experimental forest of Jinan, Shandong Province. The widely popular Willow No. 172 was used as the control. We numbered Luliu 2, Luliu 6, Jinan 1, Jinan 2, Binzhou 1, and Willow No. 172 as Sm2, Sm6, SmA, SmB, SmC, and Sm172 for this paper, respectively. The branches used in this study were collected from the experimental forest of Xicang Village, Changqing District, Jinan City, Shandong Province.

2.2. Experimental Methods

(1) Pot experiment: In April 2017, potted seedlings were cultivated with sieved soil. The soil was taken from the Forestry Experimental Station of Shandong Agricultural University. Before loading, it was screened to remove impurities and homogenized. The soil is sandy loam with a pH of 7.05 ± 0.03 , a total nitrogen content of $1.27 \pm 0.14 \text{ g} \cdot \text{kg}^{-1}$, the hydrolyzable nitrogen content of $94.36 \pm 13.89 \text{ mg} \cdot \text{kg}^{-1}$, the available phosphorus content of $32.01 \pm 4.10 \text{ mg} \cdot \text{kg}^{-1}$, the available potassium content of $56.72 \pm 7.83 \text{ mg} \cdot \text{kg}^{-1}$, and the organic matter content of $16.27 \pm 2.39 \text{ g} \cdot \text{kg}^{-1}$. The cuttings of *Salix matsudana* clones Sm6 and Sm172 were selected and planted into greenhouse flowerpots at the Forestry Experimental Station of Shandong Agricultural University. The upper diameter of the flowerpots was 30 cm, the lower diameter was 20 cm, and the height was 25 cm. The weight of the soil in each pot was 10 kg. After planting, each cutting protruded approximately 2 cm above the soil surface. Regular watering management was conducted during the study. After the cuttage seedlings survived, the weak seedlings were eliminated in July 2017, while the seedlings that grew well and had no obvious diseases and pests were selected for experiments. The greenhouse was equipped with a water curtain, fan, and other temperature control equipment. During the experiment, the day and night temperatures in the greenhouse were controlled at $(25 \pm 2) ^\circ\text{C}$ and $(20 \pm 2) ^\circ\text{C}$ respectively, and the relative humidity was 65–70%.

Soil salinity was determined by the gravimetric method. A soil salinity gradient (0.1%, 0.3%, 0.5%, and 0.7%) was prepared, and deionized water was used as the blank control. First, the mass of NaCl needed for each stress level was calculated. NaCl solutions with the corresponding concentrations were prepared in deionized water and added three times in equal amounts (irrigation once every 7 days). A tray was placed below each pot to prevent the loss of salt. The physiological and biochemical indices were measured 15 days after the last addition of the salt.

(2) Transcriptome analysis: Transcriptome sequencing was performed using a combination of second-generation and third-generation sequencing technologies. Normally growing Sm6 and Sm172 adult plants (one each) were selected. Several branches with similar growth were cut at a length of approximately 15 cm. The cuttings were placed in beakers filled with deionized water and cultivated in a constant-temperature light incubator. After the branches took root and grew new leaves, various groups of branches were soaked in $200 \text{ mmol} \cdot \text{L}^{-1}$ NaCl solution for 0, 4, 12, and 24 h. The leaves were collected from all groups immediately after the soaking treatment. During sampling, leaves were collected from 3 plants in each group and mixed. Immediately after collection, the samples were placed in liquid nitrogen and then stored in a $-80 ^\circ\text{C}$ freezer. The samples were saved for procedures such as RNA extraction.

2.3. Determination of Salt Tolerance Indices and Data Analysis

We grouped the indices related to the salt tolerance of *Salix matsudana* into four groups, salt injury indices, physiological and biochemical indices, biomass indices, and photosynthetic indices (Table 1), and used them to establish the standard equation of salt tolerance index. The root fresh weight (RFW), shoot fresh weight (SFW), relative leaf water content (RWC), relative seedling height (RH), and relative diameter (RD) were determined according to the method developed by Chen et al. [33]. The chlorophyll content was measured following Wang et al. [34]. Using a portable photosynthesis system (CIRAS-2), the net photosynthetic rate (Pn), stomatal conductance (GS), and intercellular CO_2

concentration (Ci) were measured between 9:00 a.m. and 11:00 a.m. at a saturated light intensity of $1200 \mu\text{mol}\cdot\text{m}^{-2}\cdot\text{s}^{-1}$ and a leaf chamber temperature of 25°C . The relative conductivity (RC) and malondialdehyde (MDA) content were determined as described by Qin et al. [35]. The activities of peroxidase (POD) and superoxide dismutase (SOD) were determined following Li et al., and the contents of soluble sugar (SS) and starch (SST) were determined according to Wang et al. [36,37].

Table 1. Indexes for standard equation construction.

Category	Indexes	Abbreviations	Relative Value Codes
Phenotype	Salt injury index	SII	x1
Biomass	Shoot fresh weight	SFW	x2
	Root fresh weight	RFW	x3
	Water content	RWC	x4
	Seedling height growth	RH	x5
Photosynthetic index	Ground diameter growth	RD	x6
	Net photosynthetic rate	Pn	x7
	Intercellular CO_2 concentration	Ci	x8
	Stomatal conductance	GS	x9
	Chlorophyll	Chl	x10
Physiological and biochemical index	Superoxide dismutase	SOD	x11
	Peroxidase	POD	x12
	Malondialdehyde	MDA	x13
	Conductivity	EC	x14
	Soluble sugar	SS	x15
	Soluble starch	SST	x16

All statistical analyses were conducted using Statistical Product Service Solutions for Windows 22.0 (SPSS, Chicago, IL, USA).

2.4. Sequencing Method and Analysis

Leaf RNA was extracted, and a cDNA library was constructed. Second-generation sequencing was performed on the Illumina HiSeq high-throughput sequencing platform. The third-generation full-length transcriptome sequencing was performed by Anoroad Gene Technology Co., Ltd. (Beijing, China) with the PacBio Sequel sequencer. Sequencing quality was assessed using FastQC. Functional annotation was performed with Trinotate. GO classification was performed with BLAST2GO. COG classification was performed using eggNOG. Metabolic pathway analysis was performed using the KEGG. Differential expression analysis was conducted with DESeq. The GO classification of the differentially expressed Unigene and Pathway enrichment analysis were performed using Goseq.

2.5. Verification of the Differentially Expressed Genes

RNAs were extracted from Sm6 and Sm172 that had received salt treatment for 0, 4, 12, or 24 h. The RNAs were reverse-transcribed, and 12 randomly selected salt-tolerance-related genes of *Salix matsudana* were subjected to real-time fluorescence quantitative verification. The polymerase chain reaction (PCR) system (20 μL) was set up as follows: SYBR Green 10 μL , forward primer (10 mM) 1 μL , reverse primer (10 mM) 1 μL , cDNA 2 μL , and ddH₂O to a total volume of 20 μL . The PCR conditions were as follows: predenaturation at 95°C for 30 s and 40 cycles of denaturation at 95°C for 5 s and optimal annealing temperature 60°C for 30 s.

3. Results

3.1. Comprehensive Evaluation of the Salt Tolerance of *Salix matsudana* Clones at the Seedling Stage

3.1.1. Analysis of Variance of Salt Tolerance Index between NaCl Treatment Concentration and Tree Species

Analysis of variance (Table 2) showed that all indexes showed significant or extremely significant differences under different NaCl concentrations and among different clones. Analysis of variance showed that the data of the indicators selected in this test were reliable.

Table 2. ANOVA analyses of effects of salt and clone treatments and their interaction on the growth, biomass, photosynthetic, physiological, and biochemical of *Salix matsudana*.

Variables	Salt Treatment		Clone Treatment		Salt × Clones	
	F-Value	p-Value	F-Value	p-Value	F-Value	p-Value
SFW	120.94	<0.001	8.793	<0.001	1.935	<0.05
RFW	47.081	<0.001	4.34	<0.01	2.902	<0.001
RWC	3.497	<0.05	3.898	<0.01	2.759	<0.001
RH	555.974	<0.001	16.797	<0.001	9.68	<0.001
RD	558.212	<0.001	4.719	<0.001	6.314	<0.001
Chl	249.154	<0.001	181.623	<0.001	31.436	<0.001
GS	44.091	<0.001	3.91	<0.01	1.944	<0.05
Pn	1293.128	<0.001	91.144	<0.001	11.486	<0.001
Ci	3.931	<0.01	1.539	0.191	1.141	0.336
MDA	532.732	<0.001	811.72	<0.001	40.707	<0.001
POD	97.785	<0.001	100.371	<0.001	16.692	<0.001
SOD	720.173	<0.001	818.479	<0.001	85.472	<0.001
EC	7.072	<0.001	3.505	<0.01	2.766	<0.001
SS	128.457	0 < 0.001	226.815	<0.001	66.527	<0.001
SST	0.518	0.723	4.314	<0.01	1.445	0.138

3.1.2. Analysis of the Correlation between Salt Resistance Capability and Salt Tolerance Index

Correlation analysis of the 16 indices (Table 3) showed that there were various degrees of correlation between the indices in *Salix matsudana* exposed to salt stress. The salt injury index was positively correlated with the intercellular concentrations of CO₂ and malondialdehyde and negatively correlated with stomatal conductance, net photosynthetic rate, chlorophyll, biomass, and growth weight. The range of change varied between the indices, indicating that the results might be one-sided if single indices were used to evaluate the salt tolerance of *Salix matsudana*. The salt tolerance of *Salix matsudana* is a complex comprehensive trait.

3.1.3. Grey Relational Cluster Analysis of the Indices of Various Clones

The grey correlation degree was calculated from the membership function values of the relative values of the 16 indices of the six varieties (Table 4), and the indices were subjected to cluster analysis. At a fixed critical value $r \in (0,1)$, the index x_i and the index x_j were considered to be the same type of index when $\xi_{ij} \geq r$ ($i \neq j$). In this experiment, the critical value $r = 0.57$ was used to screen out two types of index clusters: $C_1 = \{x_4, x_8, x_{11}, x_{12}, x_{14}, x_{15}, x_{16}\}$ and $C_2 = \{x_1, x_2, x_3, x_5, x_6, x_7, x_9, x_{10}, x_{13}\}$. In the above classification, leaf water content, intercellular CO₂ concentration, SOD, POD, electrical conductivity, soluble sugar, and soluble starch were classified into one category, while the salt injury index, chlorophyll content, shoot fresh weight, root fresh weight, seedling height growth, ground diameter growth, stomatal conductance, net photosynthetic rate, and malondialdehyde were classified into another category. Table 5 shows that these two types of indices contributed different amounts to the comprehensive evaluation of salt tolerance.

Table 3. Correlation coefficient of every single index.

	SII	GS	PN	CI	RWC	SFW	RFW	SOD	MDA	EC	SS	SST	Chl	POD	RH
GS	−0.760 ***														
PN	−0.911 ***	0.882 ***													
CI	0.477 **	−0.222	−0.467 **												
RWC	0.161	−0.185	−0.268	0.003											
SFW	−0.875 ***	0.744 ***	0.827 ***	−0.378 *	−0.146										
RFW	−0.776 ***	0.458 *	0.714 ***	−0.617 **	−0.139	0.666 ***									
SOD	−0.042	−0.268	−0.133	−0.038	−0.127	−0.097	0.061								
MDA	0.581 **	−0.503 **	−0.606 **	0.537 **	−0.193	−0.561 **	−0.375 *	0.019							
EC	−0.324	0.541 **	0.394 *	−0.07	−0.074	0.246	0.234	−0.505 **	−0.013						
SS	0.32	−0.445 *	−0.421 *	0.14	0.141	−0.103	−0.07	−0.02	0.229	−0.276					
SST	0.045	−0.166	−0.142	−0.071	0.035	0.092	−0.055	0.26	−0.093	−0.165	0.515 **				
Chl	−0.631 **	0.610 **	0.665 ***	−0.235	−0.108	0.658 ***	0.422 *	0.082	−0.519 **	−0.057	−0.374 *	−0.208			
POD	−0.032	−0.136	−0.095	−0.024	0.086	−0.17	0.183	0.363 *	0.303	0.012	−0.25	−0.454 *	−0.019		
RH	−0.926 ***	0.829 ***	0.914 ***	−0.338	−0.172	0.899 ***	0.668 ***	−0.023	−0.591 **	0.361	−0.364 *	−0.072	0.665 ***	−0.109	
RD	−0.948 ***	0.753 ***	0.889 ***	−0.496 **	−0.280	0.887 ***	0.712 ***	−0.018	−0.565 **	0.384 *	−0.36	0.025	0.582 **	−0.071	0.908 ***

Notes: All original data are the average value of three repetitions. Except for the salt damage index, we calculated the relative value of each index (relative value = value of salt treated material/value of control material). Salt damage level: Grade 1: the plant is strong, the leaves are flat, green, and shiny; Grade 2: the plant wilts slightly, the leaf edge turns yellow or loses water slightly; Grade 3: plants wilt, and leaves droop, shrink, and turn yellow; Grade 4: the plant is seriously wilted, and the leaves fall off or wither; Grade 5: all leaves dry or fall off. Salt damage index = Σ (number of damaged plants at all levels) \times Corresponding grade value)/(total number of plants investigated \times Maximum salt damage level value). Levels of significance are indicated by asterisks: * $p < 0.05$; ** $p < 0.01$; *** $p < 0.001$.

Table 4. Grey correlation degree of every single index.

Evaluation Item	Correlation Degree	Ranking
SOD	0.759	1
POD	0.728	2
EC	0.656	3
RWC	0.627	4
SST	0.623	5
SS	0.613	6
CI	0.574	7
RFW	0.562	8
MDA	0.554	9
RH	0.546	10
RD	0.54	11
Chl	0.537	12
SFW	0.532	13
GS	0.524	14
PN	0.523	15
SII	0.497	16

Table 5. Principal component eigenvalues, contribution rate, and cumulative contribution rate of C₁ and C₂ indicators.

Category	Indexes	Characteristic Value	Contribution Rate (%)	Cumulative Contribution Rate (%)
C ₁	Pn	7.734	85.94%	85.94%
	RH	0.431		
	SFW	0.344		
	SII	0.219		
	RD	0.106		
	GS	0.08		
	Chl	0.051		
	RFW	0.027		
	MDA	0.007		
C ₂	SOD	5.49	87.15%	87.15%
	POD	1.513		
	SST	1.245		
	SS	1.044		
	RWC	0.545		
	CI	0.354		
	EC	0.189		

3.1.4. Principal Component Analysis of the Two Types of Indices

Since the cumulative variance contribution rates of the two types of indices were both greater than 85% (85.94% and 87.15%, respectively), these indices could be subjected to principal component analysis (Table 6). To evaluate the salt tolerance of the examined varieties, the comprehensive salt tolerance value (S) of each variety was calculated from the scores of the two types of indices obtained by principal component analysis ($S = F_1 \times W_1 + F_2 \times W_2$). The scoring formula for the C₁ comprehensive indices was $F_1 = hc_1 \times yc_1$, while the scoring formula for C₂ comprehensive indices was $F_2 = hc_2 \times yc_2$. The weight coefficient of principal components (h) was generally expressed as the variance contribution rate (namely, $hc_1 = 0.8594$, $hc_2 = 0.8715$). The linear combination of principal components of the C₁ and C₂ indices was obtained through principal component analysis: $yc_1 = 0.113x_3 + 0.116x_{10} + 0.124x_5 + 0.123x_1 + 0.118x_9 + 0.121x_6 + 0.123x_2 + 0.128x_7 + 0.112x_{13}$; $yc_2 = -0.15x_8 - 0.21x_4 + 0.391x_{11} + 0.013x_{14} - 0.262x_{16} - 0.26x_{15} + 0.344x_{12}$. The weight coefficients of the index clusters ($w_1 = 0.561$ and $w_2 = 0.439$) were calculated through the analytic hierarchy process.

Table 6. Comparison of score calculated by principal components in six *Salix matsudana*.

Type	Sm6	Sm2	SmA	Sm172	SmC	SmB
F ₁	1.593892412	1.739830574	1.61428782	1.63688199	1.506493542	1.407123631
F ₂	−0.005852612	−0.393786624	−0.444860471	−0.619278358	−0.474227168	−0.518359797
S	0.891604346	0.803172624	0.71032172	0.646427597	0.636957151	0.561836407
Sort by salt S values	1	2	3	4	5	6

Notes: F₁: Score of class C₁ index; F₂: Score of class C₂ index; S: Consolidated values.

The S values are given in Table 6. On the basis of a cut-off value of 0.7, Sm6, Sm2, and SmA of the six *Salix matsudana* varieties were salt-tolerant, whereas Sm172, SmC, and SmB were salt-sensitive.

3.1.5. Screening of the Identification Indices of Salt Tolerance of *Salix matsudana* at the Seedling Stage

Using the comprehensive salt tolerance value of the six varieties and the salt-stress-related indices, a regression equation was established to identify the salt tolerance of *Salix matsudana* at the seedling stage. The equation was used to screen out the identification indices of salt tolerance at the seedling stage. An optimal regression equation was established through stepwise regression analysis using the comprehensive S value as the dependent variable and the relative values of the indices as the independent variables: $y = 0.224x_{10} + 0.216x_{11} + 0.127x_{12} + 0.191x_7 - 0.187$ ($r = 0.949$, $R^2 = 0.90$), where y is the S index, x_{10} is chlorophyll, x_{11} is SOD, x_{12} is POD, and x_7 is Pn. The regressors x_{10} , x_{11} , and x_{12} were extremely significantly correlated with y ($p = 0.009$, 0.000 , and 0.002 , respectively), while x_7 was significantly correlated with y ($p = 0.034$). According to the equation, chlorophyll, SOD, POD, and Pn could be used as key indices to identify the salt tolerance of *Salix matsudana* at the seedling stage.

3.2. Transcriptome Analysis of *Salix matsudana* under NaCl Stress

3.2.1. Classification of the *Salix matsudana* Genes That Were Differentially Expressed in Response to Salt Stress

The second-generation sequencing data were compared and quantified using the full-length transcripts as a reference. The obtained read count was compared between groups, yielding intergroup ratios. The genes with $|\log_2\text{Ratio}| \geq 1$ and $q < 0.05$ were considered significantly differentially expressed genes between two groups. The number of differential genes varied with the duration of salt treatment (Table 7). The differential genes were roughly divided into three major categories on the basis of the clustering results: 12 h salt treatment, 24 h salt treatment, and 0–4 h salt treatment (Figure 1). The results of NT, NR, and BLASTX annotation showed that a greater number of differential genes were annotated at 12 h vs. 0 h, 12 h vs. 4 h, 24 h vs. 0 h, and 24 h vs. 4 h (4362 genes on average). According to the annotation results of the major databases, more than 98.33% of genes in the NT and NR databases were annotated (Table 8).

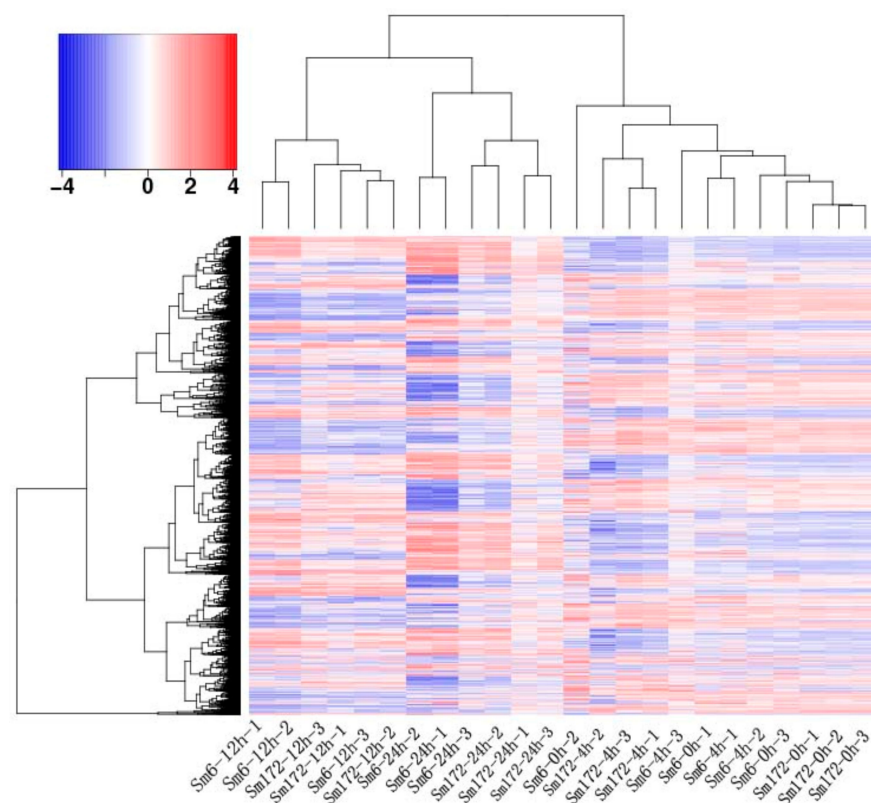
3.2.2. Pathway Analysis of the Differentially Expressed Genes

All the metabolic pathways in the KEGG were subjected to enrichment analysis using the hypergeometric test. The 20 KEGG metabolic pathways with the most significant enrichment of the differentially expressed genes were identified (Table 9), which gave us an intuitive understanding of the metabolic processes and signal transduction pathways altered in *Salix matsudana* under salt stress. More differentially expressed genes were detected after 12 h and 24 h of stress treatment, and more metabolic pathways were involved at these times, such as amino acid biosynthesis, plant hormone signal transduction, amino acid and nucleotide sugar metabolism, cysteine and methionine metabolism, mitogen-activated protein kinase (MAPK) signaling pathway, and carbon metabolism. These findings indicate that these metabolic pathways might play an important role in the salt stress response of *Salix matsudana*.

Table 7. Summary of differentially expressed genes.

Name	Up	Down	Total	Proportion
Sm172t24h-Sm172t12h	1554	674	2228	7.10%
Sm172t24h-Sm172t4h	2486	1519	4005	12.72%
Sm172t24h-Sm172t0h	1710	1118	2828	9%
Sm172t12h-Sm172t4h	1914	2515	4429	14.10%
Sm172t12h-Sm172t0h	1450	2584	4034	12.80%
Sm172t4h-Sm172t0h	223	195	418	1.30%
Sm6t24h-Sm6t12h	1795	1335	3130	9.90%
Sm6t24h-Sm6t4h	2284	2503	4787	15.20%
Sm6t24h-Sm6t0h	2494	2671	5165	16.40%
Sm6t12h-Sm6t4h	1743	3157	4900	15.60%
Sm6t12h-Sm6t0h	1977	2774	4751	15.10%
Sm6t4h-Sm6t0h	52	10	62	0.10%
Sm6t24h-Sm172t24h	48	66	114	0.30%
Sm6t12h-Sm172t12h	33	1	34	0.10%
Sm6t4h-Sm172t4h	497	253	750	2.30%
Sm6t0h-Sm172t0h	24	24	48	0.10%

Name: variance comparison combination; Up: upregulated gene; Down: downregulated gene; Total: sum of differential genes; Proportion: the proportion of significantly different genes in this group in the total different genes in this group.

**Figure 1.** Cluster map of DEGs.

3.2.3. *Salix matsudana* Genes Differentially Expressed in Response to Salt Stress and Expression Verification

Analysis of the transcriptome data revealed that *Salix matsudana* adapted to and resisted salt stress and conducted self-regulation mainly through participating in carotenoid biosynthesis, MAPK signaling, phytohormone signal transduction, flavonoid biosynthesis, starch metabolism, and sucrose metabolism. The differential genes were screened out using a multiple of difference >2 and a corrected $p < 0.01$. Among the nine differential genes with the most significant gene expression difference, *Sm172-f2p30-2392*, *Sm172-f2p28-2386*, *Sm6-*

f8p60-2372, and *Sm172-f2p39-2386* were involved in the synthesis of 9-cis-epoxycarotenoid dioxygenase (NCED) and the regulation of NCED and abscisic acid (ABA) contents. *Sm6-f2p39-2263* participated in the synthesis of asparagine synthase and positively regulated the response of *Salix matsudana* to salt stress. *Sm6-f16p60-2374* was involved in circadian rhythm and photosensitive processes. *Sm172-f3p54-1980* was involved in ABA-activated signaling pathways and was closely related to leaf senescence. *Sm6-f3p60-931*, *Sm6-f2p60-1067*, and *Sm172-f2p30-1863* were involved in MAPK metabolic pathway. *Sm6-f2p60-1067* was related to the PYL gene. It promoted the ABA signal response by inducing PYL overexpression. *Sm172-f2p30-1863* was related to the synthesis of protein phosphatase 2C (PP2C). Silencing of *Sm172-f2p30-1863* promoted the signal response of ABA. As a result of these changes, *Salix matsudana* became more sensitive to ABA and more promptly regulated its own response mechanism in the face of stress.

The expression of the nine selected genes was verified by fluorescence-based quantitative PCR. The genes numbered *Sm172-f2p30-2392*, *Sm172-f2p28-2386*, *Sm6-f8p60-2372*, *Sm6-f2p39-2263*, *Sm6-f16p60-2374*, *Sm6-f3p60-931*, *Sm6-f2p60-1067*, *Sm172-f3p54-1980*, and *Sm172-f3p54-1980* were upregulated. The change trend of the expression of the nine genes was consistent with the results of transcriptome sequencing (Figure 2).

Table 8. Gene annotations in databases.

Comparison Combinations	Annotated Number	The Proportion of Annotated Genes in Databases						
		NT	NR	BLASTX	BLASTP	PFAM	eggNOG	KEGG
Sm6t4h-Sm6t0h	62	98.39%	98.39%	88.71%	83.87%	74.19%	69.35%	41.94%
Sm6t12h-Sm6t0h	4751	99.64%	99.41%	87.77%	79.44%	73.08%	66.93%	34.50%
Sm6t12h-Sm6t4h	4900	99.61%	99.27%	87.98%	79.33%	73.08%	65.88%	33.16%
Sm6t24h-Sm6t0h	5165	99.59%	99.17%	88.02%	79.09%	73.20%	67.76%	35.28%
Sm6t24h-Sm6t4h	4787	99.56%	99.08%	87.61%	78.96%	73.05%	66.79%	33.61%
Sm6t24h-Sm6t12h	3130	99.55%	99.20%	87.73%	79.20%	70.93%	66.90%	30.83%
Sm172t4h-Sm172t0h	418	98.56%	98.33%	87.80%	78.47%	74.64%	59.33%	23.68%
Sm172t12h-Sm172t0h	4034	99.43%	99.23%	88.23%	79.33%	72.43%	66.04%	32.15%
Sm172t12h-Sm172t4h	4429	99.53%	99.32%	87.56%	79.25%	73.40%	65.39%	32.38%
Sm172t24h-Sm172t0h	2828	99.26%	98.76%	86.32%	76.59%	70.47%	65.56%	31.26%
Sm172t24h-Sm172t4h	4005	99.30%	98.90%	86.44%	77.60%	71.16%	65.99%	30.91%
Sm172t24h-Sm172t12h	2228	99.69%	99.15%	88.51%	80.30%	71.99%	66.47%	32.36%

Table 9. The top 20 KEGG pathways with the highest concentration of DEGs.

Metabolic Pathway ID	Number of DEGs in this Pathway with Annotations						Pathway Annotation
Sm6	4 h–0 h	12 h–0 h	12 h–4 h	24 h–0 h	24 h–4 h	24 h–12 h	
ko01230	0	79	67	77	60	0	Biosynthesis of amino acids
ko04075	0	0	61	79	86	55	Plant hormone signal transduction
ko00520	0	39	39	37	40	0	Amino sugar and nucleotide sugar metabolism
ko00270	0	36	32	45	36	0	Cysteine and methionine metabolism
ko04016	0	0	0	55	55	32	MAPK signaling pathway-plant
ko01200	0	0	0	73	64	0	Carbon metabolism
ko00500	0	29	33	0	32	25	Starch and sucrose metabolism
ko04712	0	36	32	0	0	32	Circadian rhythm-plant
ko00941	0	29	31	16	17	0	Flavonoid biosynthesis
ko00280	0	18	19	23	26	0	Valine, leucine, and isoleucine degradation
ko00071	0	17	21	22	24	0	Fatty acid degradation
ko00940	0	27	29	0	26	0	Phenylpropanoid biosynthesis
ko00260	0	26	0	28	26	0	Glycine, serine, and threonine metabolism
ko00561	0	20	21	0	20	16	Glycerolipid metabolism
ko00052	0	15	16	16	14	12	Galactose metabolism
ko01212	0	0	24	25	22	0	Fatty acid metabolism
ko00620	0	0	0	34	31	0	Pyruvate metabolism
ko00053	0	19	22	0	18	0	Ascorbate and aldarate metabolism
ko00592	0	20	20	0	16	0	alpha-Linolenic acid metabolism
ko00906	4	13	14	0	13	0	Carotenoid biosynthesis

Table 9. Cont.

Metabolic Pathway ID	Number of DEGs in this Pathway with Annotations						Pathway Annotation
	Sm172	4 h–0 h	12 h–0 h	12 h–4 h	24 h–0 h	24 h–4 h	
ko04075		0	56	0	80	83	Plant hormone signal transduction
ko04712		0	35	32	17	27	Circadian rhythm—plant
ko04016		0	0	0	51	54	MAPK signaling pathway—plant
ko00500		0	34	27	20	0	Starch and sucrose metabolism
ko00940		0	29	24	18	24	Phenylpropanoid biosynthesis
ko00941		8	25	27	0	24	Flavonoid biosynthesis
ko00270		0	0	37	19	31	Cysteine and methionine metabolism
ko01230		0	0	69	0	0	Biosynthesis of amino acids
ko00561		0	18	17	15	0	Glycerolipid metabolism
ko00073		0	17	19	9	0	Cutin, suberine, and wax biosynthesis
ko00906		0	17	14	10	0	Carotenoid biosynthesis
ko00592		0	0	14	13	13	alpha-Linolenic acid metabolism
ko00280		0	0	16	13	17	Valine, leucine, and isoleucine degradation
ko00450		0	11	13	10	11	Selenocompound metabolism
ko00196		0	20	15	9	0	Photosynthesis—antenna proteins
ko00944		3	10	13	0	11	Flavone and flavonol biosynthesis
ko00945		0	11	9	6	8	Stilbenoid, diarylheptanoid, and gingerol biosynthesis
ko00330		0	0	0	16	18	Arginine and proline metabolism
ko00030		0	0	20	13	0	Pentose phosphate pathway
ko04626		0	0	0	0	32	Plant–pathogen interaction

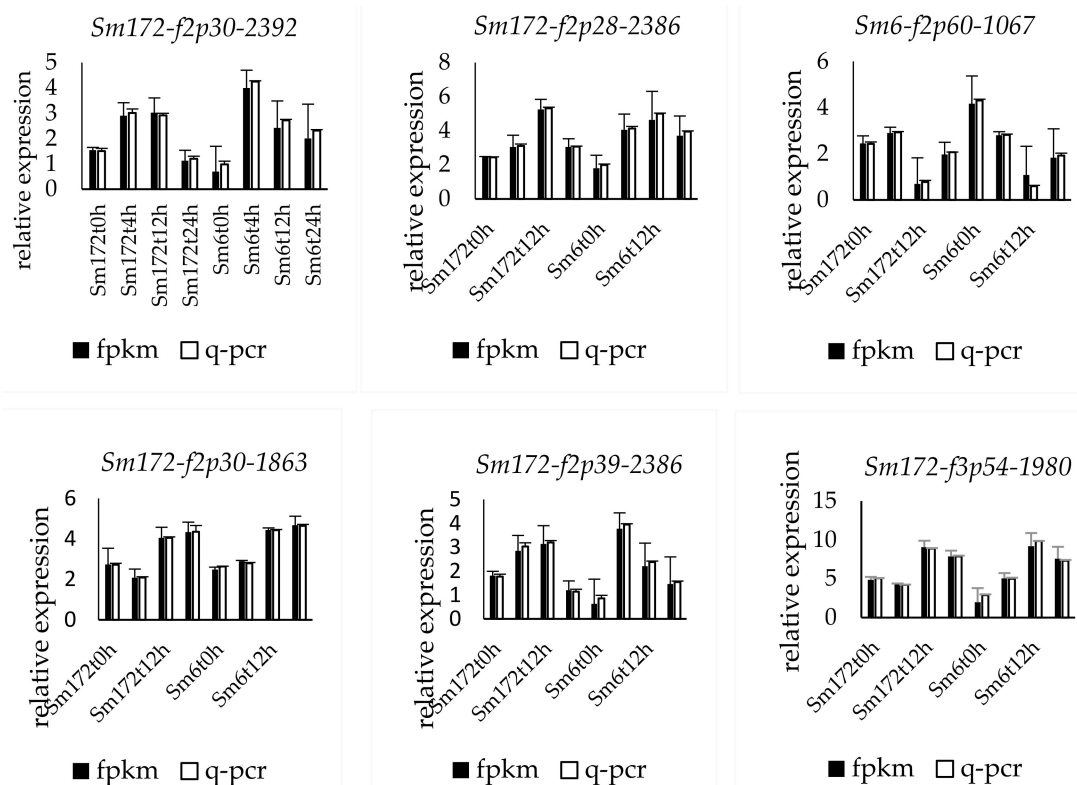


Figure 2. Cont.

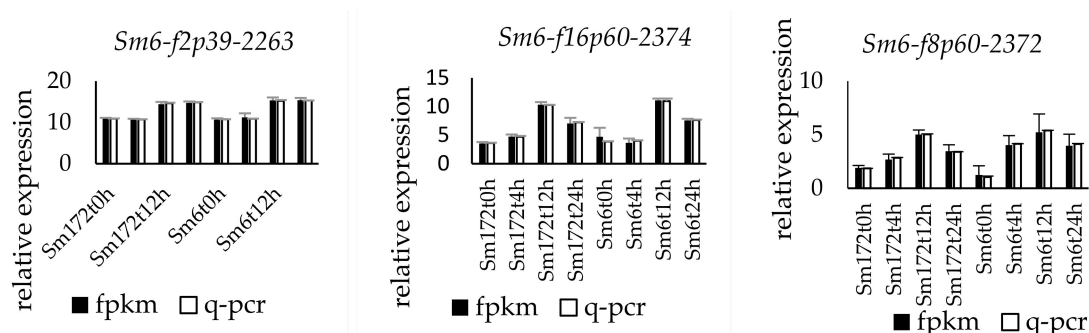


Figure 2. Expression profiles of 9 key DEGs in two poplar cultivars. Note: Sm172 stands for willow 172; Sm6 stands for Luliu 6.

4. Discussion

This study analyzed the chosen indices using a combination of the analytic hierarchy process and principal component analysis, which was more reasonable than directly doing principal component analysis on all indices. SOD, POD, chlorophyll, and net photosynthetic rate may be used as key indices to identify the salt tolerance of *Salix matsudana* at the seedling stage [38–40]. Upon salt stress, the antioxidant enzymes such as SOD and POD were activated in all clones of *Salix matsudana*, which led to the elimination of the toxicity of free radicals. SOD prevents the formation of free radicals and the damage to cells mainly by regulating the content of $O_2^{\cdot-}$. It is the first line of defense against cell damage [39,41]. POD plays an important role in protecting cells from H_2O_2 stress [42]. In response to salt stress, photosynthesis is reduced in *Salix matsudana*. The accumulation of photosynthetic products is inhibited, which hinders the growth and development of plants and even causes plant death [43]. As an important photosynthetic pigment, chlorophyll plays an important role in absorption, transmission, and transformation of light energy [3,44,45]. Therefore, the change in chlorophyll content is an important index of plant growth [46]. Salt stress leads to ion toxicity, hinders the absorption of Mg^{2+} by plants, blocks the synthesis of chlorophyll, reduces chlorophyll content, and thus seriously hinders photosynthesis [47–51]. Such findings are consistent with the research results of Gong et al. [52,53].

Under salt stress, reactive oxygen species activate a variety of MAPK signaling cascades, inducing specific cellular responses. This study found that in *Salix matsudana* exposed to salt stress, the most strongly expressed MAPK signaling pathway was the mitogen-activated protein kinase (MPK). This study showed that H_2O_2 phosphorylated mitogen-activated protein kinase kinase 4/5 (MKK4/5) by activating ANP1 upstream of the MPK cascade, thereby phosphorylating MPK3. This result is consistent with the findings of Kim et al. [54] and Kovtun et al. [55]. H_2O_2 also directly activated MPK3 by inducing the formation of nucleoside diphosphate kinase 2 (NDPK2), in line with the findings of Moon et al. [56]. The serine-threonine protein kinase OX11 (oxidative-signal-inducible 1) was also activated by peroxide and responded through the downstream MPK3. In the process of cell death caused by reactive oxygen species through the above three pathways, MPK3 is significantly upregulated, and the level of reactive oxygen species (such as H_2O_2) is increased [57], which eventually leads to cell death. When *Salix matsudana* is exposed to low salt stress or short-term salt stress, the upregulation of MPK3 and the increase in H_2O_2 lead to elevated activities of SOD and POD in the antioxidant system, which allows the resistance to the damage of reactive oxygen species and maintenance of normal physiological function of cells. Therefore, improving the activity of antioxidant enzymes in plants and increasing the level of plant antioxidant metabolism are important ways to enhance the salt tolerance of plants. Alleviation of the harm of salt stress to *Salix matsudana* could be achieved by inhibiting the expression of the MPK3-related gene Sm6-f3p60-931, which suppressed the activity of MPK3 and inhibited the production of reactive oxygen species. This biological process played a certain positive role in the salt stress resistance of

Salix matsudana and provided evidence that SOD and POD are key indices of salt tolerance in *Salix matsudana*.

In addition, this study showed that MPK3 of the MAPK pathway cascade was significantly upregulated under salt stress, which reduced the function of *SPEECHLESS* (*SPCH*) and inhibited stomatal development. The basic helix-loop-helix (*bHLH*)-type transcription factors that regulate stomatal development include three members: *SPCH*, *MUTE*, and *FAMA*. These proteins are involved in the regulation of the initiation of the M cell lineage, the formation of guard mother cells, and the symmetrical division of guard mother cells [58,59]. *SPCH* has a region between the *bHLH* domain and the C-terminal region that is rich in the acidic amino acids serine and threonine. It mediates the direct phosphorylation of *SPCH* by MPK3 [60–62], which hinders stomatal development and directly hinders photosynthesis. Therefore, physiological study of *Salix matsudana* showed that, with more concentrated or longer salt treatment, the net photosynthetic rate was reduced in each *Salix matsudana* clone. This finding provides evidence that the net photosynthetic rate is a key index of salt tolerance in *Salix matsudana*.

Moreover, genes with large differences in expression levels are involved in the synthesis of *NCED*. According to the metabolic pathway map of carotenoid biosynthesis, carotenoid biosynthesis is related to ABA synthesis [54,63]. ABA plays a central role in plant responses to stressful environments [64,65]. In the process of ABA synthesis, zeaxanthin epoxidase catalyzes the conversion of carotene to violaxanthin. *NCED* further catalyzes the conversion of 9-cis-flavin to xanthotoxin, which further leads to the production of abscisic aldehyde. Abscisic aldehyde is eventually converted into ABA under the action of an amine oxidase. These findings are consistent with the results of Li et al. [23]. *NCED* is a member of the carotenoid cleavage dioxygenase family. It is the most important rate-limiting enzyme in the process of ABA biosynthesis in higher plants and belongs to a class of key genes involved in the regulation of ABA biosynthesis [66,67]. *NCED* expression level is positively correlated with ABA content in plants [68–70]. Therefore, the goal of plant physiological self-regulation might be achieved through the control of the expression of *NCED* synthesis-related genes such as *Sm172-f2p28-2386*, *Sm172-f2p30-2392*, *Sm172-f2p39-2386*, and *Sm6-f8p60-2372*, which further control the expression of *NCED* and regulate the content of ABA in plants. In future research on the salt tolerance of *Salix matsudana*, ABA might become a key index.

These data provide a scientific basis for future research on the mechanism of *Salix matsudana* salt tolerance, deliver a simpler method for the identification and breeding of salt-tolerant *Salix matsudana* varieties, and can guide the selection of salt-tolerant tree species in the coastal saline-alkali land of the Yellow River Delta.

Author Contributions: Conceptualization, Y.P. and B.C.; formal analysis, P.M.; investigation, Y.G., W.L. and X.C.; data curation, T.W. and L.G.; writing—original draft preparation, Y.P.; writing—review and editing, P.M. and B.C.; visualization, L.G.; supervision, B.C.; funding acquisition, B.C. All authors have read and agreed to the published version of the manuscript.

Funding: This research was funded by the Central Finance Forestry Reform and Development Fund (Forestry Science and Technology Promotion Demonstration Subsidy) ([2020]TG08), the Major Scientific and Technological Innovation in Shandong (2017CXGC0316), and the National Forestry Public Welfare Industry Research Project (201404107).

Institutional Review Board Statement: Not applicable.

Informed Consent Statement: Not applicable.

Data Availability Statement: Not applicable.

Conflicts of Interest: The authors declare no conflict of interest.

References

- Liu, P.; Bai, J.; Ding, Q.; Shao, H.; Gao, H.; Xiao, R. Effects of Water Level and Salinity on TN and TP Contents in Marsh Soils of the Yellow River Delta, China. *CLEAN—Soil Air Water* **2012**, *40*, 1118–1124. [\[CrossRef\]](#)
- Liu, S.; Hou, X.; Yang, M.; Cheng, F.; Coxixio, A.; Wu, X.; Zhang, Y. Factors driving the relationships between vegetation and soil properties in the yellow river delta, china. *Catena* **2018**, *165*, 279–285. [\[CrossRef\]](#)
- Xia, J.; Ren, J.; Zhang, S.; Wang, Y.; Fang, Y. Forest and grass composite patterns improve the soil quality in the coastal saline-alkali land of the yellow river delta, china. *Geoderma* **2019**, *349*, 25–35. [\[CrossRef\]](#)
- Li, B.; Ouyang, J.; Wang, J.; Wu, H.; Liu, X.; Zou, J. Effects of NaCl on seedling growth and some physiological characteristics of *Salix matsudana* Koidz. *J. Tianjin Norm. Univ.* **2017**, *37*, 37–42.
- Dimitriou, I.; Aronsson, P.; Weih, M. Stress tolerance of five willow clones after irrigation with different amounts of landfill leachate. *Bioresour. Technol.* **2006**, *97*, 150–157. [\[CrossRef\]](#)
- Wang, Y.; Yuan, H.W.; Li, M.; Li, Y.J.; Ma, X.J.; Tan, F.; Zhang, J. Phenotypic and physiological responses of two willow varieties to salt stress. *Isr. J. Plant Sci.* **2013**, *61*, 73–82. [\[CrossRef\]](#)
- Yang, Y.; Yan, G. Elucidating the molecular mechanisms mediating plant salt-stress responses. *New Phytol.* **2018**, *217*, 523–539. [\[CrossRef\]](#)
- Hasegawa, P.M. Sodium (Na^+) homeostasis and salt tolerance of plants. *Environ. Exp. Bot.* **2013**, *92*, 19–31. [\[CrossRef\]](#)
- Munns, R.; Tester, M. Mechanisms of salinity tolerance. *Annu. Rev. Plant Biol.* **2008**, *59*, 651–681. [\[CrossRef\]](#)
- Zhang, M.; Smith, J.A.C.; Harberd, N.P.; Jiang, C. The regulatory roles of ethylene and reactive oxygen species (ROS) in plant salt stress responses. *Plant Mol. Biol.* **2016**, *91*, 651–659. [\[CrossRef\]](#)
- Foyer, C.H.; Shigeoka, S. Understanding oxidative stress and antioxidant functions to enhance photosynthesis. *Plant Physiol.* **2011**, *155*, 93–100. [\[CrossRef\]](#) [\[PubMed\]](#)
- Meloni, D.A.; Oliva, M.A.; Martinez, C.A.; Cambraia, J. Photosynthesis and activity of superoxide dismutase, peroxidase and glutathione reductase in cotton under salt stress. *Environ. Exp. Bot.* **2003**, *49*, 69–76. [\[CrossRef\]](#)
- Barba-Espín, G.; Clemente-Moreno, M.J.; Álvarez, S.A.; García-Legaz, M.F.; Hernández, J.A.; Díaz-Vivancos, P. Salicylic acid negatively affects the response to salt stress in pea plants. *Plant Biol.* **2011**, *13*, 909–917. [\[CrossRef\]](#) [\[PubMed\]](#)
- Qiao, G.; Zhang, X.; Jiang, J.; Liu, M.; Han, X.; Yang, H.; Zhuo, R. Comparative proteomic analysis of responses to salt stress in chinese willow (*Salix matsudana koidz*). *Plant Mol. Biol. Rep.* **2014**, *32*, 814–827. [\[CrossRef\]](#)
- Zhou, J. *Changes of miRNA Expression in Populus Euphratica and Salix Mandshurica under Salt Stress*; Chinese Academy of Forestry: Beijing, China, 2010.
- Chen, Y.; Jiang, Y.; Chen, Y.; Feng, W.; Liu, G.; Yu, C.; Lian, B.; Zhong, F.; Zhang, J. Uncovering candidate genes responsive to salt stress in *Salix matsudana* (koidz) by transcriptomic analysis. *PLoS ONE* **2020**, *15*, e0236129. [\[CrossRef\]](#)
- Shan, L.; Zhao, S.; Xia, G. Research Progress on the Identification of Salt-tolerance Related Genes and Molecular Mechanism on Salt Tolerance in Higher Plants. *Mol. Plant Breed.* **2006**, *4*, 15.
- Yang, H.B.; Dung, C.H.; Xu, X.F.; Wang, Y.; Han, Z.H. Effects of NaCl and Iso-osmotic polyethylene glycol stress on Na^+/H^+ antiport activity of three malus species with different salt tolerance. *J. Integr. Agric.* **2014**, *13*, 1276–1283. [\[CrossRef\]](#)
- Yang, Y.Q.; Han, X.L.; Ma, L.; Wu, Y.J.; Liu, X.; Fu, H.Q.; Liu, G.Y.; Lei, X.G.; Guo, Y. Dynamic changes of phosphatidylinositol and phosphatidylinositol 4-phosphate levels modulate H^+ -atpase and Na^+/H^+ antiporter activities to maintain ion homeostasis in arabidopsis under salt stress. *Mol. Plant* **2021**, *14*, 2000–2014. [\[CrossRef\]](#)
- Filiz, E.; Kurt, F. Expression and co-expression analyses of WRKY, MYB, bHLH and bZIP transcription factor genes in potato (*Solanum tuberosum*) under abiotic stress conditions: RNA-seq data analysis. *Potato Res.* **2021**, *64*, 721–741. [\[CrossRef\]](#)
- Das, A.; Pramanik, K.; Sharma, R.; Gantait, S.; Banerjee, J. In-silico study of biotic and abiotic stress-related transcription factor binding sites in the promoter regions of rice germin-like protein genes. *PLoS ONE* **2019**, *14*, e0211887. [\[CrossRef\]](#)
- Mokhtari, F.; Rafiei, F.; Shabani, L.; Shiran, B. Differential expression pattern of transcription factors across annual medicago genotypes in response to salinity stress. *Biol. Plant.* **2017**, *61*, 227–234. [\[CrossRef\]](#)
- Li, H.; Li, D.F.; Chen, A.G.; Tang, H.J.; Li, J.J.; Huang, S.Q. RNA-seq for comparative transcript profiling of kenaf under salinity stress. *J. Plant Res.* **2017**, *130*, 365–372. [\[CrossRef\]](#) [\[PubMed\]](#)
- Okay, S.; Derelli, E.; Unver, T. Transcriptome-wide identification of bread wheat wrky transcription factors in response to drought stress. *Mol. Genet. Genom.* **2014**, *289*, 765–781. [\[CrossRef\]](#) [\[PubMed\]](#)
- Meng, C.; Quan, T.Y.; Li, Z.Y.; Cui, K.L.; Yan, L.; Liang, Y.; Dai, J.L.; Xia, G.M.; Liu, S.W. Transcriptome profiling reveals the genetic basis of alkalinity tolerance in wheat. *BMC Genom.* **2017**, *18*, 24. [\[CrossRef\]](#) [\[PubMed\]](#)
- Kumar, S.; Kanakachari, M.; Gurusamy, D.; Kumar, K.; Narayanasamy, P.; Venkata, P.K.; Solanke, A.; Gamanagatti, S.; Hiremath, V.; Katageri, I.S.; et al. Genome-wide transcriptomic and proteomic analyses of bollworm-infested developing cotton bolls revealed the genes and pathways involved in the insect pest defence mechanism. *Plant Biotechnol. J.* **2016**, *14*, 1438–1455. [\[CrossRef\]](#)
- Zhang, F.; Zhu, G.; Du, L.; Shang, X.; Cheng, C.; Yang, B.; Hu, Y.; Cai, C.; Guo, W. Genetic regulation of salt stress tolerance revealed by RNA-seq in cotton diploid wild species, *Gossypium davidsonii*. *Sci. Rep.* **2016**, *6*, 20582. [\[CrossRef\]](#)
- Chen, M.-S.; Zhao, M.-L.; Wang, G.-J.; He, H.-Y.; Bai, X.; Pan, B.-Z.; Fu, Q.-T.; Tao, Y.-B.; Tang, M.-Y.; Martínez-Herrera, J.; et al. Transcriptome analysis of two inflorescence branching mutants reveals cytokinin is an important regulator in controlling inflorescence architecture in the woody plant *Jatropha curcas*. *BMC Plant Biol.* **2019**, *19*, 468. [\[CrossRef\]](#)

29. Goyal, E.; Amit, S.K.; Singh, R.S.; Mahato, A.K.; Chand, S.; Kanika, K. Transcriptome profiling of the salt-stress response in *Triticum aestivum* cv. Kharchia local. *Sci. Rep.* **2016**, *6*, 27752. [[CrossRef](#)]
30. Amirbakhtiar, N.; Ismaili, A.; Ghaffari, M.R.; Firouzabadi, F.N.; Shobbar, Z.S.; Jain, M. Transcriptome response of roots to salt stress in a salinity-tolerant bread wheat cultivar. *PLoS ONE* **2019**, *14*, e0213305. [[CrossRef](#)]
31. Tian, X.; Wang, Z.; Zhang, Q.; Huacong, C.; Wang, P.; Lu, Y.; Jia, G.; Sara, A. Genome-wide transcriptome analysis of the salt stress tolerance mechanism in *Rosa chinensis*. *PLoS ONE* **2018**, *13*, e0200938. [[CrossRef](#)]
32. Xie, R.; Pan, X.; Zhang, J.; Ma, Y.; He, S.; Zheng, Y.; Ma, Y. Effect of salt-stress on gene expression in citrus roots revealed by RNA-seq. *Funct. Integr. Genom.* **2017**, *18*, 155–173. [[CrossRef](#)] [[PubMed](#)]
33. Chen, Y.; Li, C.; Lei, C.; Yi, J.; Gong, M. Identification and Comprehensive Evaluation of Drought Tolerance in Diploid Potato, *S. phureja* Germplasm Resources. *Mol. Plant Breed.* **2019**, *17*, 3416. [[CrossRef](#)]
34. Wang, Z.; Li, M.; Hao, R.L.; Chen, L.Q.; Han, Y.Q.; Zhang, B. Comparison of photosynthetic characteristics of broomcorn millet spike mutants. *J. Shanxi Agric. Sci.* **2020**, *48*, 879–883. [[CrossRef](#)]
35. Qin, Y. Study on Cold Resistance of Introduced Ornamental Bamboo Species in Shandong Province. Master's Thesis, Shandong Agricultural University, Tai'an, China, 2014.
36. Li, H.S. *Principles and Techniques of Plant Physiological and Biochemical Experiments*; Higher Education Press: Beijing, China, 2000; pp. 164–165.
37. Wang, X.Y.; Wang, S.L.; Tang, Y.; Zhou, W.M.; Zhou, L.; Zhong, Q.L.; Dai, L.M.; Yu, D.P. Characteristics of non-structural carbohydrate reserves of three dominant tree species in broadleaved Korean pine forest in Changbai mountain, China. *Chin. J. Appl. Ecol.* **2019**, *30*, 1608–1614. [[CrossRef](#)]
38. Yu, C.W.; Guan, Z.Q.; Hong, Y.L.; Wu, Y.J.; Wang, C.; Liu, G.F.; Yang, C.P. Enhanced salt tolerance of transgenic poplar plants expressing a manganese superoxide dismutase from tamarix androssowii. *Mol. Biol. Rep.* **2010**, *37*, 1119–1124. [[CrossRef](#)]
39. Foyer, C.H.; Noctor, G. Redox signaling in plants. *Antioxid. Redox Signal.* **2013**, *18*, 2087–2090. [[CrossRef](#)]
40. Kravchik, M.; Bernstein, N. Effects of salinity on the transcriptome of growing maize leaf cells point at cell-age specificity in the involvement of the antioxidative response in cell growth restriction. *BMC Genom.* **2013**, *14*, 24. [[CrossRef](#)]
41. Amor, N.B.; Jiménez, A.; Megdiche, W.; Lundqvist, M.; Sevilla, F.; Abdelly, C. Response of antioxidant systems to NaCl stress in the halophyte *Salicornia maritima*. *Physiol. Plant.* **2010**, *126*, 446–457. [[CrossRef](#)]
42. Chaparadeh, N.; D'Amico, M.L.; Khavari-Nejad, R.A.; Izzo, R.; Navari-Izzo, F. Antioxidative responses of *Calendula officinalis* under salinity conditions. *Plant Physiol. Biochem.* **2004**, *42*, 695–701. [[CrossRef](#)]
43. Yang, J.Y.; Zheng, W.; Tian, Y.; Wu, Y.; Zhou, D.W. Effects of various mixed salt-alkaline stresses on growth, photosynthesis, and photosynthetic pigment concentrations of medicago ruthenica seedlings. *Photosynthetica* **2011**, *49*, 275–284. [[CrossRef](#)]
44. Wu, Y.; Jin, X.; Liao, W.; Hu, L.; Dawuda, M.M.; Zhao, X.; Tang, Z.; Gong, T.; Yu, J. 5-aminolevulinic acid (ALA) alleviated salinity stress in cucumber seedlings by enhancing chlorophyll synthesis pathway. *Front. Plant Sci.* **2018**, *9*, 635. [[CrossRef](#)] [[PubMed](#)]
45. Huihui, Z.; Yue, W.; Xin, L.; Guoqiang, H.; Yanhui, C.; Zhiyuan, T.; Jieyu, S.; Nan, X.; Guangyu, S. Chlorophyll synthesis and the photoprotective mechanism in leaves of mulberry (*Morus alba* L.) seedlings under NaCl and NaHCO₃ stress revealed by tmt-based proteomics analyses. *Ecotoxicol. Environ. Saf.* **2020**, *190*, 110164. [[CrossRef](#)] [[PubMed](#)]
46. Koldobika, H.; Maria, B.J.; Isabel, F.; Marta, P.; Ignacio, G.-P.J. Functional role of red (*retro*)-carotenoids as passive light filters in the leaves of *Buxus sempervirens* L.: Increased protection of photosynthetic tissues? *J. Exp. Bot.* **2005**, *56*, 2629–2636. [[CrossRef](#)]
47. Mukhtar, E.; Siddiqi, E.H.; Bhatti, K.H.; Nawaz, K.; Hussain, K. Gas exchange attributes can be valuable selection criteria for salinity tolerance in canola cultivars (*Brassica napus* L.). *Pak. J. Bot.* **2013**, *45*, 35–40.
48. Ye, L.; Zhao, X.; Bao, E.C.; Cao, K.; Zou, Z.R. Effects of arbuscular mycorrhizal fungi on watermelon growth, elemental uptake, antioxidant, and photosystem II activities and stress-response gene expressions under salinity-alkalinity stresses. *Front. Plant Sci.* **2019**, *10*, 863. [[CrossRef](#)]
49. Guo, R.; Zhou, J.; Ren, G.X.; Hao, W. Physiological responses of linseed seedlings to iso osmotic polyethylene glycol, salt, and alkali stresses. *Agron. J.* **2013**, *105*, 764–772. [[CrossRef](#)]
50. Guo, R.; Zhou, J.; Hao, W.P.; Gu, F.X.; Liu, Q.; Li, H.R.; Xia, X.; Mao, L.L. Germination, growth, chlorophyll fluorescence and ionic balance in linseed seedlings subjected to saline and alkaline stresses. *Plant Prod. Sci.* **2014**, *17*, 20–31. [[CrossRef](#)]
51. He, Q. The Ionic Response and Physiological Ecological Changes of *Ph.Praecox* under Salt Stress. Ph.D. Thesis, Chinese Academy of Forestry, Beijing, China, 2011.
52. Gong, B.; Wen, D.; Vanderlangenberg, K.; Wei, M.; Yang, F.; Shi, Q.; Wang, X. Comparative effects of NaCl and NaHCO₃ stress on photosynthetic parameters, nutrient metabolism, and the antioxidant system in tomato leaves. *Entia Hortic.* **2013**, *157*, 1–12. [[CrossRef](#)]
53. Hui-Hui, Z.; Guang-Liang, S.; Jie-Yu, S.; Xin, L.; Ma-Bo, L.; Liang, M.; Nan, X.; Guang-Yu, S. Photochemistry and proteomics of mulberry (*Morus alba* L.) seedlings under NaCl and NaHCO₃ stress. *Ecotoxicol. Environ. Saf.* **2019**, *184*, 109624. [[CrossRef](#)]
54. Kim, S.H.; Woo, D.H.; Kim, J.M.; Lee, S.Y.; Chung, W.S.; Moon, Y.H. Arabidopsis MKK4 mediates osmotic-stress response via its regulation of MPK3 activity. *Biochem. Biophys. Res. Commun.* **2011**, *412*, 150–154. [[CrossRef](#)]
55. Kovtun, Y.I.; Chiu, W.L.; Tena, G.; Sheen, J. Functional analysis of oxidative stress-activated mitogen-activated protein kinase cascade in plants. *Proc. Natl. Acad. Sci. USA* **2000**, *97*, 2940–2945. [[CrossRef](#)]

56. Moon, H.; Lee, B.; Choi, G.; Shin, S.; Prasad, D.T.; Lee, O.; Kwak, S.S.; Kim, D.N.J.; Bahk, J.; Hong, J.C. NDP kinase 2 interacts with two oxidative stress-activated MAPKs to regulate cellular redox state and enhances multiple stress tolerance in transgenic plants. *Proc. Natl. Acad. Sci. USA* **2003**, *100*, 358–363. [[CrossRef](#)] [[PubMed](#)]
57. Su, J.; Yang, L.; Zhu, Q.; Wu, H.; He, Y.; Liu, Y.; Xu, J.; Jiang, D.; Zhang, S. Active photosynthetic inhibition mediated by MPK3/MPK6 is critical to effector-triggered immunity. *PLoS Biol.* **2018**, *16*, e2004122. [[CrossRef](#)] [[PubMed](#)]
58. Macalister, C.A.; Ohashi-Ito, K.; Bergmann, D. Transcription factor control of asymmetric cell divisions that establish the stomatal lineage. *Nature* **2007**, *445*, 537–540. [[CrossRef](#)] [[PubMed](#)]
59. Morales-Navarro, S.; Pérez-Díaz, R.; Ortega, A.; Marcos, A.D.; Mena, M.; Fenoll, C.; González-Villanueva, E.; Ruiz-Lara, S. Overexpression of a *sdd1*-like gene from wild tomato decreases stomatal density and enhances dehydration avoidance in arabidopsis and cultivated tomato. *Front. Plant Sci.* **2018**, *9*, 940. [[CrossRef](#)] [[PubMed](#)]
60. Lampard, G.R.; Lukowitz, W.; Ellis, B.E.; Bergmann, D.C. Novel and expanded roles for mapk signaling in arabidopsis stomatal cell fate revealed by cell type-specific manipulations. *Plant Cell* **2009**, *21*, 3506–3517. [[CrossRef](#)]
61. Zhang, Y.; Guo, X.; Dong, J. Phosphorylation of the polarity protein BASL differentiates asymmetric cell fate through MAPKS and SPCH. *Curr. Biol.* **2016**, *26*, 2957–2965. [[CrossRef](#)]
62. Samakovli, D.; Ticha, T.; Vavrdova, T.; Ovecka, M.; Luptovciak, I.; Zapletalova, V.; Kucharova, A.; Krennek, P.; Krasnylenko, Y.; Margaritopoulou, T. Yoda-hsp90 module regulates phosphorylation-dependent inactivation of speechless to control stomatal development under acute heat stress in arabidopsis. *Mol. Plant Engl. Version* **2020**, *13*, 612–633. [[CrossRef](#)]
63. Wang, Y.H.; Que, F.; Li, T.; Zhang, R.R.; Khadr, A.; Xu, Z.S.; Tian, Y.S.; Xiong, A.S. DcABF3, an ABF transcription factor from carrot, alters stomatal density and reduces ABA sensitivity in transgenic *arabidopsis*. *Plant Sci.* **2021**, *302*, 110699. [[CrossRef](#)]
64. Hasegawa, P.M.; Bressan, R.A.; Zhu, J.K.; Bohnert, H.J. Plant cellular and molecular responses to high salinity. *Annu. Rev. Plant Physiol. Plant Mol. Biol.* **2000**, *51*, 463–499. [[CrossRef](#)]
65. Finkelstein, R.R.; Gampala, S.; Rock, C.D. Absciscic acid signaling in seeds and seedlings. *Plant Cell* **2002**, *14* (Suppl. S1), S15–S45. [[CrossRef](#)] [[PubMed](#)]
66. Kitahata, N.; Ito, S.; Kato, A.; Ueno, K.; Nakano, T.; Yoneyama, K.; Yoneyama, K.; Asami, T. Abamine as a basis for new designs of regulators of strigolactone production. *J. Pestic. Sci.* **2011**, *36*, 53–57. [[CrossRef](#)]
67. Zhao, J.; Li, J.; Zhang, J.; Chen, D.; Qin, G. Genome-wide identification and expression analysis of the carotenoid cleavage oxygenase gene family in five rosaceae species. *Plant Mol. Biol. Rep.* **2021**, *39*, 739–751. [[CrossRef](#)]
68. Li, Q.H.; Yu, X.T.; Chen, L.; Zhao, G.; Li, S.Z.; Zhou, H.; Dai, Y.; Sun, N.; Xie, Y.F.; Gao, J.S.; et al. Genome-wide identification and expression analysis of the NCED family in cotton (*Gossypium hirsutum* L.). *PLoS ONE* **2021**, *16*, e0246021. [[CrossRef](#)]
69. Milosavljevic, A.; Prokic, L.; Marjanovic, M.; Stikic, R.; Sabovljevic, A. The effects of drought on the expression of TAO1, NCED and EIL1 genes and ABA content in tomato wild-type and flacca mutant. *Arch. Biol. Sci.* **2012**, *64*, 297–306. [[CrossRef](#)]
70. Awan, S.Z.; Chandler, J.O.; Harrison, P.J.; Sergeant, M.J.; Bugg, T.D.H.; Thompson, A.J. Promotion of germination using hydroxamic acid inhibitors of 9-cis-epoxycarotenoid dioxygenase. *Front. Plant Sci.* **2017**, *8*, 357. [[CrossRef](#)] [[PubMed](#)]